A&A manuscript no.
(will be inserted by hand later)

NASA-CR-200250

Your thesaurus codes are:
missing; you have not inserted them

ASTRONOMY
AND
ASTROPHYSICS
2.11.1995

Timing the Geminga Pulsar with EGRET Data

J.R. Mattox[1,4], J.P. Halpern[2], and P.A. Caraveo[3]

[1] Department of Astronomy, University of Maryland, College Park, MD 20742, USA
[2] Department of Astronomy, Columbia University, 538 West 120th Street, New York, NY 10027, USA
[3] Istituto di Fisica Cosmica del CNR, Via Bassini, 15, 20133 Milano, Italy
[4] e-mail: mattox@astro.umd.edu; WWWeb: http://www.astro.umd.edu/~mattox/

Received; accepted

Abstract. The pulsation of Geminga has been detected to date only at high energies (E > 0.1 keV). Since X-ray exposures are short and Geminga is at best only marginally detected in γ-rays at E< 30 MeV, the primary means of timing Geminga is with high-energy γ-rays. The EGRET observations of Geminga now span 4 years. These data are analyzed to determine the 1995 ephemeris for Geminga which is provided here. We continue to count every revolution of Geminga during the GRO mission with a rotational phase resolution which improves with additional exposure. Proper motion is now apparent in γ-ray timing, consistent with the optical measurement of Bignami *et al.* (1993). With improved statistics, two additional peaks are tentatively detected in the "minor bridge" region. More exposure is required to confirm them. If found to be real, they are difficult to understand with polar cap models, but are expected for the outer gap model, and provide sorely needed constraints.

1. Introduction

The high-energy γ-ray source "Geminga" is now known to be a rotation-powered pulsar with period $P = 0.237$ s, surface magnetic field $B_p \sim 1.6 \times 10^{12}$ G, and spin-down age $\tau = P/2\dot{P} = 3.4 \times 10^5$ yr. It is the second brightest high-energy γ-ray source in the sky, and the only known radio-quiet pulsar despite deep searches (e.g., Seiradakis 1992). Geminga was first seen by SAS-2 (Thompson *et al.* 1977) and studied extensively by COS-B (Bennett *et al.* 1977). An unusual soft X-ray source (1E 0630+178) detected by the Einstein Observatory in the COS-B error box (Bignami *et al.* 1983) later turned out to be the correct counterpart. An optical candidate (G″) which was the bluest object in the field was found within the Einstein error box (Bignami *et al.* 1987; Halpern & Tytler 1988). The ROSAT detection of periodic X-ray emission from 1E 0630+178 (Halpern & Holt 1992) with a period of 237 ms lead to a successful search for periodicity in the nearly contemporaneous EGRET data (Bertsch et al. 1992), as well as in the archival COS-B (Bignami & Caraveo 1992; Hermsen *et al.* 1992) and SAS-2 data (Mattox *et al.* 1992). Proper motion of the G″ star has been detected (Bignami, Caraveo, & Mereghetti 1993), establishing it as the correct optical counterpart. Caraveo *et al.* (1995) have recently reported the detection with the Hubble Space Telescope of a parallactic displacement of G″ of $0''.0064 \pm 0''.0017$. The corresponding distance is 157^{+59}_{-34} pc.

Although the existence of high-energy periodicity was initially established with ROSAT data (Halpern & Holt 1992), the primary means of timing Geminga is with high-energy γ-rays because X-ray exposures are short and the X-ray peaks are broad. After the work of Bertsch *et al.* (1992), the growing EGRET database has been analysed by Mayer-Hasselwander *et al.* (1994) and Mattox *et al.* (1994). Thanks to new pointed EGRET observations that have substantially increased the number of γ-ray events as well as the time span of the EGRET database, we can provide an improved ephemeris for Geminga. The method is more fully described by Mattox *et al.* (1994). More complete Geminga timing results and their interpretation will be published elsewhere.

2. The Derivation of the 1995 Ephemeris for Geminga

As described by Mattox *et al.* (1994), the ephemeris parameters are estimated as the values which give the largest value of the Z^2_n statistic (i.e., the most non-uniform light curve). Again, 10 harmonics are used, $n = 10$. Figure 1 shows the "window function" for this timing analysis. Data from cycle 4 viewing periods 412 & 413 are used along with all all EGRET data from cycles 1–3. With this 3.9 year timing interval, the minimum resolvable second derivative of frequency, $\ddot{f}$ is $\sim T^{-3} = 5.4 \times 10^{-25}$. This corresponds to a braking index $f\ddot{f}/\dot{f}^2 = 60$ which is much higher than the value of 3 expected for spin down due only

to magnetic dipole radiation. Therefore, $\ddot{f}$ is assumed to be zero. Because the estimates of the ephemeris parameters f and $\dot{f}$ are correlated, they are obtained by a grid search. The estimate of f and $\dot{f}$ given in Table 1 is the point where Z^2_{10} is maximum. There is one clear maximum. For illustration, the dependence on f with $\dot{f}$ fixed at the value which maximizes Z^2_{10} is shown in Figure 2. Since this peak stands out clearly in both f and $\dot{f}$, we are confident that we are counting every revolution of Geminga during the GRO era. As an additional confirmation, Mattox *et al.* (1994) note that the phase for each observation (in observation cycles 1 and 2) was consistent with the ephemeris thus derived.

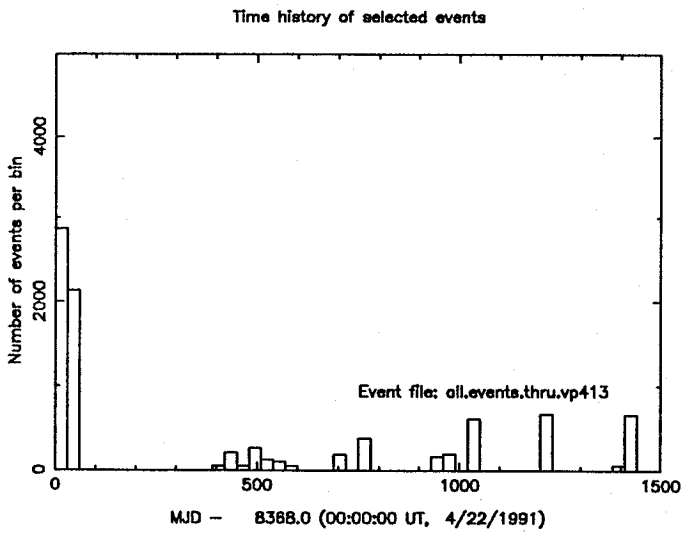

Fig. 1. The history of EGRET observations of Geminga portrayed through a histogram of arrival times.

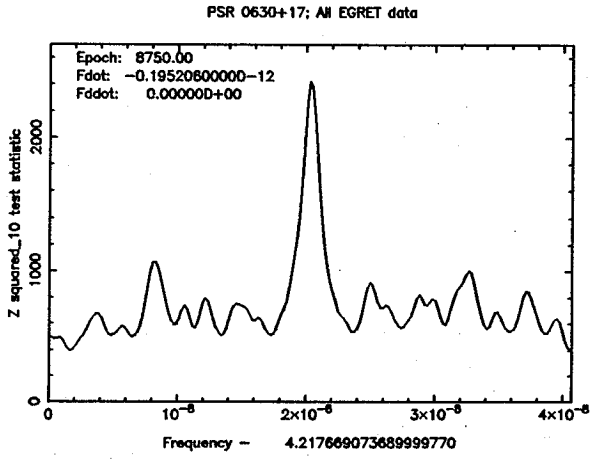

Fig. 2. The dependence of Z^2_{10} on f with $\dot{f}$ fixed.

The "1995 EGRET Geminga Ephemeris" shown in Table 1 was thus obtained. The uncertainties of the estimated values of f and $\dot{f}$ are defined by the interval in which Z^2_{10} decreases by 5.1 from the maximum value. A bootstrap calculation described in the Mattox *et al.* (1994) indicates that this decrease corresponds to the 95% confidence interval.

The uncertainty of f is a factor of 2 smaller than the "1993 EGRET Geminga Ephemeris" given in Mattox *et al.* (1994). This level of improvement is expected, since the time span was extended by a factor of 1.8 over the 2.1 years which separate the beginning of cycle 1 and the last cycle 2 observation. The uncertainty of $\dot{f}$ is similarly a factor of 4 smaller since it is resolved in proportion to the square of the length of the timing interval. From the sharpness of the peaks obtained with this ephemeris (see figure 3), we conclude that the phase is correct to within 0.02 revolutions for the timespan of the EGRET observations used here (1991–1995). Beyond this timespan, the decay of the accuracy of the phase prediction (assuming no glitch) is dominated by the uncertainty of $\ddot{f}$:

$$\Delta\phi = 0.02[\frac{T-1993}{2\ \mathrm{yr}}]^3 \qquad (1)$$

If it is assumed that Geminga has not glitched between the COS-B and the EGRET observations, the second derivative of frequency can be estimated from the change in $\dot{f}$ from $-1.95238(2)\times10^{-13}$ Hz/s in the Hermsen *et al.* (1992) ephemeris to the value in Table 1. Since 410 million seconds separate the epochs of the ephemerides, the estimate is $\ddot{f} = (8\pm1)\times10^{-26}\mathrm{Hz/s^2}$. The corresponding braking index, $f\ddot{f}/\dot{f}^2$, is 9 ± 1. This is significantly higher than the value of 3 expected for magnetic dipole radiation. If this is a true braking index, it implies that rotational energy is extracted more efficiently than expected, a very interesting finding which is very important for understanding the Geminga pulsar magnetosphere. A reanalysis of the COS-B data using the a more accurate position and proper motion is required to confirm this result.

3. The Effect of Position Error on Timing

For a pulsar timing analysis, EGRET event times are transformed to the arrival times at the solar system barycenter. The time delay is $\boldsymbol{\zeta}\cdot\boldsymbol{D}/c$, where $\boldsymbol{\zeta}$ is the direction assumed for the pulsar, and $\boldsymbol{D}$ is the vector from the barycenter to GRO. If $\boldsymbol{\zeta}$ is in error by $\boldsymbol{\delta}$, the calculated barycenter arrival time will be in error by $\boldsymbol{\delta}\cdot\boldsymbol{D}/c$. The maximum possible error is

$$\delta_e\frac{|\boldsymbol{D}|}{c} = 2.3\frac{\delta_e}{1''}\ \mathrm{ms}, \qquad (2)$$

where δ_e is the component of $\boldsymbol{\delta}$ in the plane of the ecliptic. With sensitivity to phase errors of order 10^{-2} in timing

Epoch: T0 = 2448750.5 JD
(which is 1992 May 8.0 Barycentric Dynamical Time)
Frequency at epoch: $f = 4.21766909403(5)$ Hz
Frequency derivative: $\dot{f} = -1.95206(4) \times 10^{-13}$ Hz/s
2nd frequency derivative: $\ddot{f} = 0$ Hz/s^2)
Position: $\alpha_{2000} = 6^h33^m54^s.10$, $\delta_{2000} = +17°\ 46'\ 12''.1$
If phase zero occurs at T0, peak one is at phase 0.98(1).
If phase zero occurs at 1992 May 8.0 UTC at the geocenter, peak one is at phase 0.65(1)

Table 1. The 1995 EGRET ephemeris for GEMINGA. The 2nd frequency derivative and position are assumed. The digit in parenthesis following the derived parameters is the 95% confidence uncertainty of the last digit. See the caption of Figure 3 for a definition of peak one.

Geminga with EGRET, position errors of $\sim 1''$ are important. Indeed, Mattox *et al.* (1994) demonstrate with a 2.1 year timing interval that EGRET timing constrains Geminga to be within $1''$ of the G$''$ star in the direction of right ascension, and $8''$ in declination.

The detection of the proper motion of the G$''$ star through optical measurement (Bignami, Caraveo, & Mereghetti 1993; Mignani, Caraveo, & Bignami 1994) is very important to our work. The position specified in Table 1 is that of G$''$ at the epoch of the ephemeris. With the 2.1 year timing interval, Mattox *et al.* (1994) were not able to detect this proper motion. However, in a 3.9 year timing interval, the proper motion is detectable, as it causes the timing residuals to be twice as large, and because of improved phase resolution through more abundant statistics. When we use the proper motion of Bignami, Caraveo, & Mereghetti (1993), the maximum Z^2_{10} value increases by 25. The light curve thus obtained is shown as the upper histogram in Figure 3. It has slightly sharper peaks than the light curve obtained with a fixed position (the lower histogram in Figure 3). This result constitutes an independent confirmation that G$''$ is Geminga. The values of f and $\dot{f}$ estimated assuming the proper motion do not change from the values in Table 1. The uncertainty of $\dot{f}$ decreases by 25%.

To obtain the best timing solution for Geminga, a precise knowledge of Geminga's absolute position and proper motion is needed. Although the Hubble Space Telescope has done relative astrometry for Geminga with a precision of $\sim 0''.002$ (Caraveo *et al.* 1995), the absolute precision is limited by the $1''$ precision of the HST Guide Star Catalog. This is not enough for our purposes. Therefore, dedicated astrometric observations have been scheduled at the Torino observatory. They are expected to provide position of the field stars to within $0''.1$. This will allow the absolute optical position of Geminga to be determined to $0''.1$.

The error in the ecliptic plane component of proper motion from ground based observations (Mignani, Caraveo, & Bignami 1994) is 0.04 $''$/yr. For the 24 year baseline of EGRET, COS-B, and SAS-2, this amounts to a possible position error of $1''$ in the plane of the ecliptic, which will definitely affect γ-ray timing. The recent Hubble Space Telescope observations of Caraveo *et al.* (1995) also improve the precision of the determination of proper motion by a factor of 7.

We will ultimately attempt to link the phases and count cycles between EGRET, COS-B, and SAS-2. A coherent analysis over this 24 year baseline would produce a very precise ephemeris to support future studies at other wavelengths. Also, it would allow for a precise characterization of the timing noise and possibly allow the braking index to be measured.

In contrast to proper motion, any parallactic displacements is inconsequential to the timing of Geminga. For a distance of 157 pc (Caraveo *et al.* 1995), timing residuals from parallax will be only 14 μs, which is less than 10^{-4} cycles — entirely undetectable.

4. The Pulse Profile

The improved statistics and timing solution are evident in Figure 3 when it is compared to Mattox *et al.* (1994) for the 2.1 year interval. A strong difference in the shapes of the main peaks is emerging. Also, the asymmetry of the second peak is now apparent — its decline is sharper than its rise. Such detail will improve with further observation and will be very useful for constraining models of the emission.

From an analysis of the spatial distribution of the events in the "minor bridge" region (see the caption of Figure 3 for a definition), it is apparent that Geminga is also emitting at this phase (Fierro 1995). The marginal indication for structure in this interval seen with 2.1 years of exposure (Mattox *et al.* 1994) has become a striking feature in Figure 3. Two secondary peaks are apparent at phases 0.94 and 0.01 (defining phase 0 as the center of the minor bridge). When a smooth concave fit is made to the emission rate in the minor bridge region, these peaks deviate from the fit at the 5σ level. Because a substantial numbers of "trials" are made in choosing features a posteriori, we consider this a tentative result which needs to be confirmed with the help of late cycle 4 and cycle 5 exposure.

If found to be real, these additional peaks are difficult to understand with polar cap models, but are expected for the outer gap model. In the latter theory, a pair of outer gaps is each responsible for generating a pair of oppositely directed γ-ray beams which parallel the magnetic field lines (see Figure 8 of Halpern & Ruderman 1993). Therefore, an observer can potentially see as many as four

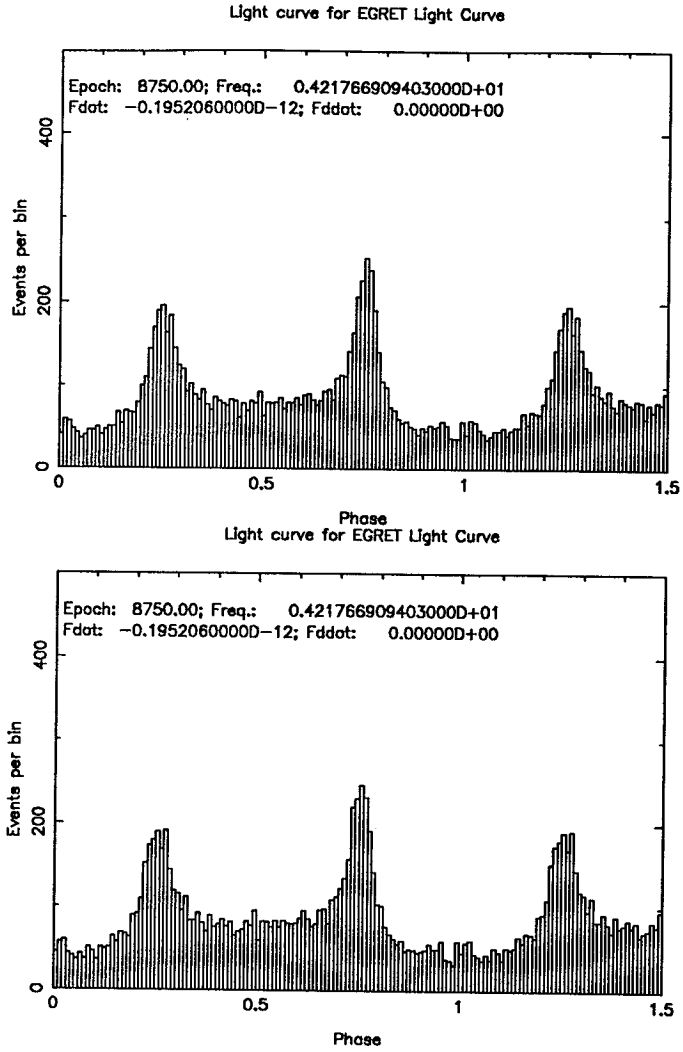

Fig. 3. The phase dependence of the Geminga γ-rays. For the top histogram, the proper motion has been used for the Barycenter correction. For the bottom histogram, the fixed position of table 1 has been used. A phase offset of 0.27 has been added to that obtained from Table 1 for the purpose of display so that peak one is at phase 0.25. Peak one precedes the strongest emission bridge, the "major bridge" region. The "minor bridge" region follows peak two. The histograms contain 8794 events from cycles 1, 2, 3, and VPs 412&413 from cycle 4. The events were selected from an energy dependent cone encompassing 68% of the point spread function at each energy, and with E> 70 MeV.

pulses whose arrival times are determined by relativistic aberation and time-of-flight delays across the magnetosphere. Detailed numerical simulations by Romani & Yadigaroglu (1995) indicate that the inward going beams are much weaker than the outward going ones. Perhaps these inward directed beams are responsible for these possible weak peaks in the minor bridge region. If so, they can be used to constrain the viewing direction, the geometry of the outer gap emission, and therefore the net γ-ray efficiency of Geminga.

Acknowledgements. J. Mattox acknowledges support from NASA Grant NAG 5-2833 and J. Halpern from NAG 5-2051.

References

Bennett, K. *et al.* 1977, A&A 56, 469.
Bertsch, D.L. *et al.* 1992, Nature 357, 306.
Bignami, G.F., Caraveo, P.A., & Lamb, R.C. 1983, ApJ 272, L9.
Bignami, G.F., Caraveo, P.A., Paul, J.A., Salotti, L. & Vigroux, L., 1987, ApJ 319.
Bignami G.F. & Caraveo P.A., 1992, Nature 357, 287.
Bignami, G.F., Caraveo, P.A., & Mereghetti, S. 1993, Nature 361, 704.
Caraveo, P.A., Bignami, G.F., Mignani, R., Taff, L.G., submitted
Fierro, J.M., 1995, Ph.D. Thesis, Stanford University
Halpern, J.P. & Tytler, D. 1988, ApJ 330, 201.
Halpern, J.P. & Holt, S.S. 1992, Nature 357, 222.
Halpern, J.P. & Ruderman, M. 1993, ApJ 415, 286.
Hermsen, W. *et al.* 1992, IAU Circular 5541.
Mattox, J.R., *et al.* 1992, ApJ 401, L23.
Mattox, J.R., *et al.* 1994, Proceedings of the 2nd GRO Symposium, AIP Conf. Proc. #304, p. 77.
Mayer-Hasselwander, H., *et al.* 1994, ApJ 421, 276
Mignani, R., Caraveo, P.A., & Bignami, G.F. 1994, The Messenger (ESO), 76, 32.
Romani, R.W., & Yadigaroglu, I.A., 1995, ApJ 438, 314.
Seiradakis, J.H., 1992, IAU Circ 5532.
Thompson, D.J. *et al.* 1977, ApJ 213, 252.

This article was processed by the author using Springer-Verlag LaTeX A&A style file *L-AA* version 3.